

The Comparisons and Analysis of Octagonal and Hexagonal Photonic Crystal Fiber for Flatness Dispersion Application

Nguyen Hoang Hai

Department of Telecommunication System, Hanoi University of Science and Technology

Email: hai.nguyenhoang@hust.edu.vn

Abstract - This paper presents an analysis and comparisons photonic crystal fibers with both the octagonal and hexagonal structures for flatness dispersion managed applications. Management of chromatic dispersions in photonic crystal structures is a very important attempt for optical transmission systems, in both the linear and nonlinear regimes, and for any optical system supporting ultra-short soliton pulse propagation. It has been shown through numerical simulation results that using a four-ring octagonal lattices structure, ultra-flattened dispersion is of 0 ± 0.50 ps/(nm-km) within a 1.31 to 1.70 μm wavelength range (390 nm band). Confinement loss is as low as 0.001 dB/km within a 1.31 to 1.65 μm wavelength ranges. A four ring hexagonal lattices structure can assume near zero ultra-flattened dispersion of 0 ± 0.10 ps/nm/km in the wavelength range of 1.45 μm to 1.75 μm (300 nm) or, 0 ± 0.51 ps/nm/km in a 1.40 to 2.0 μm (600 nm) with low confinement loss of less than 10-3 dB/m below 1.70 μm .

Keywords - Photonic crystal fiber, flattened dispersion, confinement loss.

I. INTRODUCTION

Photonic crystal fibers (PCFs) have been attracted much scientific and technological interest in recent years. Broadly speaking, PCFs may be defined as optical fibers in which the core and/or cladding regions consist of micro-structured rather than homogeneous materials. The most common type of PCF, which was first fabricated in 1996, consists of a pure silica fiber with an array of air holes running along the longitudinal axis. In conventional optical fibers, electromagnetic modes are guided by total internal reflection in a core region whose refractive index is raised by doping of the base material. In PCFs, two distinct guiding mechanisms are possible: the guided modes may be trapped in a core with a higher average index than the cladding region by an

effect similar to total internal reflection (often termed modified total internal reflection, or just index guiding), or they can be trapped in a core of lowered average index by a photonic band-gap effect. The existence of two different guiding mechanisms is one of the reasons for the versatile nature of PCFs.

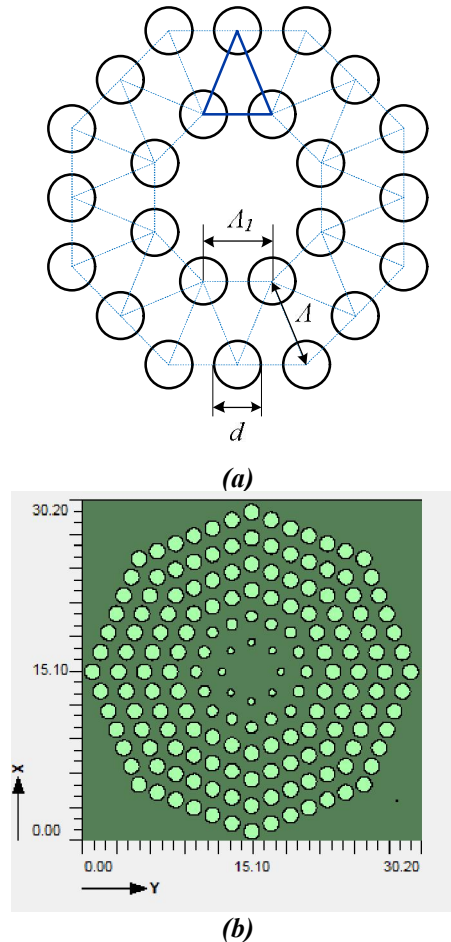


Figure 1. Cross-section geometry with three rings of air-holes of (a) O-PCF, and (b) DF-OPCF.

The chromatic dispersion in optical fibers is a very important problem for communication systems, in both the linear and nonlinear regimes, and for any optical system supporting ultra-short soliton pulse propagation [1]. In all cases, almost flattened dispersion behavior is a crucial issue. For example, in ultra-short optical soliton dispersion-managed systems the existence of non-negligible third order dispersion can lead to strong instabilities that destroy soliton pulse transmission features [2]. In the same way, it has been shown that the most suitable dispersion profile for flat and wideband supercontinuum generation in optical fibers is given by small normal dispersion and negligible third order dispersion [3]. Unlike in DWDM systems it is essential to maintain a uniform response in the different wavelength channels, which requires ultra-flattened dispersion and, moreover, with moderately low dispersion to minimize four wave mixing nonlinearities effects [4]. In all cases, the efficiency of the system depends greatly on the degree of flatness of the fiber dispersion. Fortunately, unlike the conventional step index fibers, photonic crystal fibers offer more flexibility to tune dispersion profile effectively for specific application. In this context, following sections describe novel dispersion-flattened PCFs based on the octagonal and hexagonal structures.

II. DISPERSION FLATTENED PROPERTIES OF PCF WITH OCTAGONAL LATTICES

A. The proposed octagonal lattices and design parameter.

Recently, octagonal PCFs (O-PCFs) have been reported to have significantly wider single-mode wavelength range, more circular-like field distribution around the core, inherently high nonlinearity, and lower confinement loss than conventional H-PCFs [5, 6]. Despite these attractive features, dispersion management of O-PCFs has not been studied yet. Therefore, as part of ongoing efforts to locate a novel PCF structure, in this section investigation is made on a defected ring O-PCF (hereinafter DF-OPCF) for ultra-flattened chromatic dispersion and low confinement losses.

Figure 1(a) shows a simple O-PCF geometry with optimized air-hole diameters d and pitch Λ , and Figure 1(b) shows the geometry of a DF-OPCF in APSS with one defected ring that has relatively small air-hole diameters d_l . The air-hole diameters on the

other rings are d . Core diameter a equals $2\Lambda - d_{\text{first ring}}$. The spacing between air-holes on the same ring is Λ_1 , which is related to Λ by relation $\Lambda_1 \approx 0.765\Lambda$. In contrast to a conventional H-PCF, octagonal PCFs have isosceles triangular unit lattices with a vertex angle of 45° . Due to such lattices, O-PCFs contain more air-holes in the cladding region with the same numbers of rings than H-PCFs. In O-PCFs, the total number of air-holes for rings 1, 2, 3, 4, and 5 are respectively 8, 24, 48, 80, and 120, whereas in a regular triangular lattice, the number of air-holes is 6, 18, 36, 60, and 90, respectively. This results in a higher air-filling ratio and a lower refractive index around the core, thereby providing strong confinement ability. As there are eight air holes on the first ring and is placed in an octagonal rotational symmetry, O-PCF results in similar fundamental field distribution as that of the standard step index fibers [5]. Since periodicity in the cladding region is not essential to confine the guiding light in the high index core region [7], we propose a DF-OPCF that can assume ultra-flattened dispersion and low confinement loss.

B. Numerical investigation and simulation results

The fiber is simulated by a Finite Difference Method (FDM) with Perfect Matched Layer (PML) absorbing boundary condition [6]. For numerical calculations, Cartesian co-ordinate is utilized and the background material is pure silica with refractive index 1.45. To model the leakage, an open boundary condition is used, which produces no reflection at the boundary. PMLs are so far the most efficient absorption boundary condition for this purpose. The chromatic dispersion $D(\lambda)$ is easily calculated from the second derivative of the mode index, with respect to wavelength λ . The $D(\lambda)$ parameter can be numerically calculated as [7]:

$$D(\lambda) = -\frac{\lambda}{c} \frac{d^2 \text{Re}[n_{\text{eff}}]}{d\lambda^2} \quad (1)$$

in [ps/(nm-km)], where c is the velocity of light in vacuum, is the real part of the refractive index. λ is the wavelength in units of μm . The confinement loss, L_c , can be calculated from the imaginary part of the mode index using the following equation [6]:

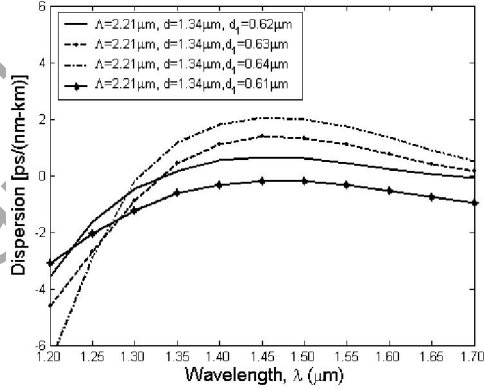
$$L_c = 8.686k_0 \text{Im}[n_{\text{eff}}] \quad (2)$$

where $\text{Im}[n_{\text{eff}}]$ is imaginary part of the effective mode index. The effective mode area is another important

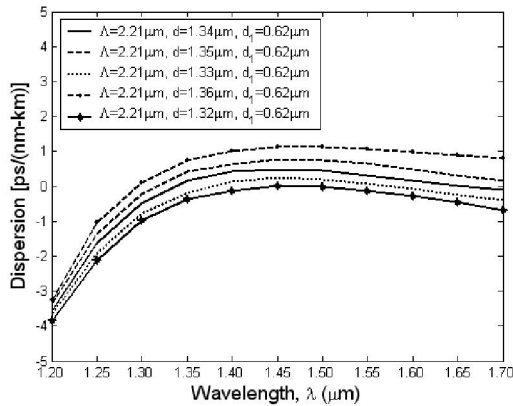
parameter for fiber design. The effective area of fiber is calculated as follows [6]:

$$A_{\text{eff}} = \frac{(\iint |E|^2 dx dy)^2}{\iint |E|^4 dx dy} \quad (3)$$

in $[\mu\text{m}^2]$, where E is the propagating electrical field.



(a)



(b)

Figure 2. Wavelength response of chromatic dispersion of the DF-OPCF in both the x and y polarization directions for (a) variations in the diameter d_1 , and (b) variations in the diameter d

In the design for DF-OPCF, four rings are used with one defected ring with air-hole diameter d_1 , as shown in Fig.1(b). The dispersion properties of the DF-OPCF are shown in Fig. 2 with a pitch and two different air-hole diameters, d_1 and d . For $\Lambda = 2.21 \mu\text{m}$, $d = 1.34 \mu\text{m}$, and $d_1 = 0.62 \mu\text{m}$, flattened dispersion of $0 \pm 0.50 \text{ ps}/(\text{nm}\cdot\text{km})$ is obtained (solid line) in the 1.31 to $1.70 \mu\text{m}$ wavelength range, since in a standard fiber draw, 1% variations in fiber diameters

may occur [8]. Therefore, to account for this structural variations air-hole diameter d is varied between 1.32 to $1.36 \mu\text{m}$, d_1 is varied between 0.6 to $0.64 \mu\text{m}$, and Λ is varied from 2.20 to $2.22 \mu\text{m}$, in Figs. 2(a), (b), and Fig. 3 respectively.

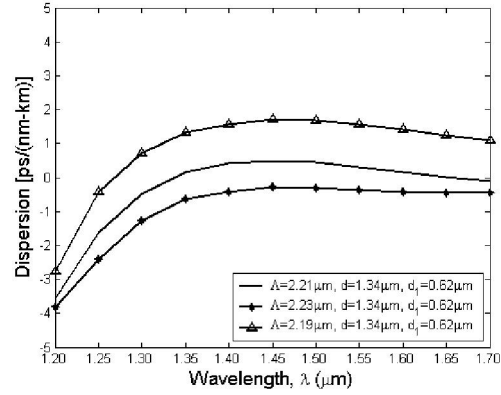


Figure 3. Wavelength response of chromatic dispersion of DF-OPCF in x and y polarization directions for variations in pitch Λ

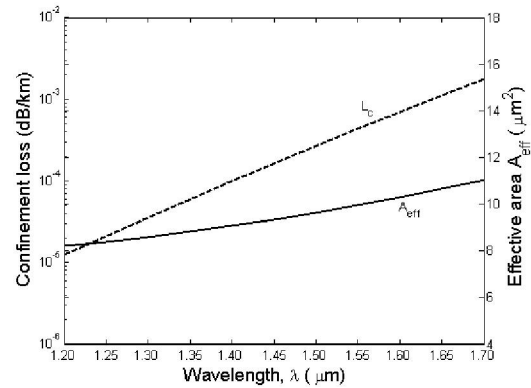


Figure 4. Wavelength response of confinement loss and effective area of DF-OPCF with four rings, $\Lambda = 2.21 \mu\text{m}$, $a = 3.80 \mu\text{m}$, $d = 1.34 \mu\text{m}$, and $d_1 = 0.62 \mu\text{m}$

The dispersion parameters are found to be more sensitive to variations in d_1 and less sensitive to variations in d . A variation of $\pm 0.01 \mu\text{m}$ in d causes a corresponding average variation in dispersion of about $\pm 0.29 \text{ ps}/(\text{nm}\cdot\text{km})$ and for the same variations in d_1 , average dispersion variation is about $\pm 0.78 \text{ ps}/(\text{nm}\cdot\text{km})$ at $1.55 \mu\text{m}$ wavelength. Again, a variation of $\pm 0.01 \mu\text{m}$ in Λ causes a corresponding average variation in dispersion of about $\pm 1.42 \text{ ps}/(\text{nm}\cdot\text{km})$. In [9], it has been reported that air hole diameters in the first ring, d_1 has significant effects on both the

dispersion magnitude and slope. An increase in d_1 causes dispersion parameter to decrease more and the dispersion slope changes rapidly. In ref. [10], it has been reported that a very small variation in the center air hole diameter also causes significant changes in both the dispersion magnitude and slope. On the other hand, Figs. 2 and 3 shows that overall response of the DF-OPCF to variation in diameter, d_1 is attracting in comparison to [9, 10]. A small variation in d_1 does not affect the magnitude and the slope of dispersion parameter too much. But, variations in d and Λ cause similar dispersion variation as has been reported for the H-PCF. Therefore, a DF-OPCF may not so sensitive to changes in the diameter of air holes on the first ring. As the effect of variations in air hole diameters on the higher order rings is not significant, it can be assumed that the proposed DF-OPCF may have better tolerance to changes in design parameters.

Figure 4 shows the wavelength dependence of DF-OPCF confinement loss with $\Lambda = 2.21 \mu\text{m}$, $d = 1.34 \mu\text{m}$, and $d_1 = 0.62 \mu\text{m}$. Confinement loss is found to be less than a 0.001 dB/km within the considered wavelength ranges despite having only four rings. This is due to the fact that when using one defected ring with smaller hole diameters, the hole diameters required for the other rings are larger, which ultimately results in a higher air-filling ratio and causes higher index difference between the core and holey cladding. Fig. 8.4 also shows that the effective area of DF-OPCF for $\Lambda = 2.21 \mu\text{m}$, $d = 1.34 \mu\text{m}$, and $d_1 = 0.62 \mu\text{m}$ is $9.6 \mu\text{m}^2$ at $1.55 \mu\text{m}$ wavelength. The nonlinear coefficient at $1.55 \mu\text{m}$ is about $10 \text{ W}^{-1}\text{Km}^{-1}$.

Figure 5 depicts the electric field for x polarization mode at $1.55 \mu\text{m}$ wavelength. Due to the small diameters of the air-holes on the first ring, the field penetrates outside the first ring, resulting in a relatively larger effective area of $9.6 \mu\text{m}^2$. Notice that the field has been confined tightly within the second ring since no leakage is evident outside the second ring. PCFs with such a small effective area, flattened dispersion, and low confinement loss can find their way in different applications, such as optical parametric amplification and supercontinuum generation in the infrared. It is found that the DF-OPCF supports a second order mode around $1.50 \mu\text{m}$. But the fiber can effectively operate as a single mode fiber in the telecommunication windows as the confinement loss of this second mode is higher than a 20 dB/km above $1.50 \mu\text{m}$ wavelength.

Two apparent advantages of the proposed topology is that firstly, DF-OPCF can assume lower cladding effective refractive index due to increased number of air holes on each ring, this result in a very low confinement loss. Secondly, by changing diameter of air holes on the first ring only, ultra-flattened chromatic dispersion in broadband range is obtained. Moreover, for DF-OPCF submicron adjustments may not require that often impose fabrication challenges.

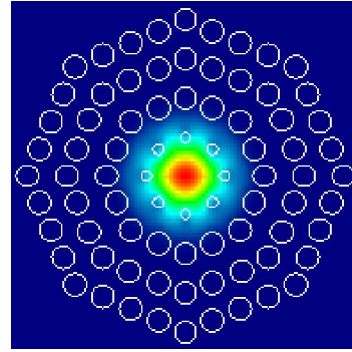


Figure 5. Fundamental mode field distribution at $\lambda = 1.55 \mu\text{m}$ with four rings, $\Lambda = 2.21 \mu\text{m}$, $a = 3.80 \mu\text{m}$, $d = 1.34 \mu\text{m}$, and $d_1 = 0.62 \mu\text{m}$.

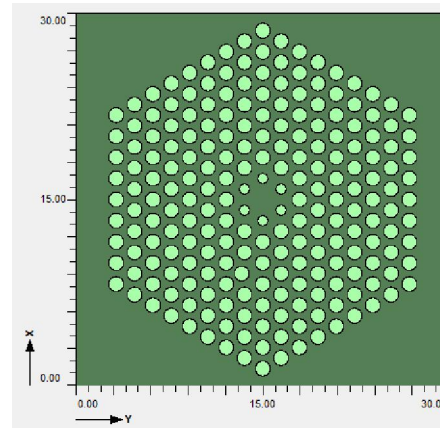


Fig. 6. The proposed DF-PCF structure with four rings. Diameter of air-holes on the first ring is d_1 , that of second to fourth rings is d_2 , and air-hole pitch is Λ .

III. THE PROPOSED HEXAGONAL LATTICES AND DESIGN PARAMETERS

Figure 6 shows a simple geometry of the proposed dispersion flattened PCF (hereinafter DF-PCF) with optimized air-hole diameters d_1 , d_2 , and pitch Λ . Since periodicity in the cladding region is not essential to confine the guiding light in the high index core region [10], air-hole diameter on the first ring is scaled down to shape dispersion property while diameter of air-holes on outer rings are kept larger for better field confinement. The present technique of modulating air-hole dimension in order to achieve suitable dispersion characteristics is also used in [7, 11], but indeed it is important to utilize the technique to explore the best possible result. A PCF design in [7] contains many design parameters that may impose great fabrication challenges. Again PCF design in [11] results a reduction in design parameters, but it causes relatively larger effective area ($13.2 \mu\text{m}^2$) and high confinement losses which is not so attractive for applications as a nonlinear media. On the other hand, we have shown successfully in the present design that modulating air-hole diameter of only the first ring is sufficient to achieve near zero ultra-flattened dispersion and low confinement loss in a broad range of wavelengths.

A. Numerical investigation and simulation results of compared hexagonal photonic crystal structure

Figure 7 shows wavelength dependence of chromatic dispersion of the proposed DF-PCF for optimum design parameters. Optimizing the parameters d_1 , d_2 , and Λ ultra-flat chromatic dispersion of $0 \pm 0.10 \text{ ps/nm/km}$ is obtained (solid line) in the wavelength range of $1.45 \mu\text{m}$ to $1.75 \mu\text{m}$ for $\Lambda = 1.70 \mu\text{m}$, $d_1/\Lambda = 0.30 \mu\text{m}$, and $d_2/\Lambda = 0.67 \mu\text{m}$. For optimization of the parameters a simple technique is applied. First a relative air-hole dimension d_2/Λ is chosen in the range of 0.5 to 0.8. Larger value is chosen for better field confinement. Then a value of d_1/Λ is calculated by examining the dispersion curves. It is known that in a standard fiber draw, $\pm 1\%$ variations in fiber global diameter may occur [8] during the fabrication process. Therefore, roughly an accuracy of $\pm 2\%$ may require ensuring dispersion flatness [9]. To account for this structural variation air-hole diameters d_1 and d_2 are varied up to $\pm 5\%$ from their optimum values. Corresponding dispersion curves are shown in Figs. 8(a) and 8(b) respectively. While d_1 is varied d_2 and Λ are kept constant and while d_2 is varied d_1 and Λ are kept constant respectively. It is found that the DF-PCF maintains dispersion flatness within $0 \pm 2.0 \text{ ps/nm/km}$ for variation of d_1 and d_2 up to $\pm 2\%$. Figure 9 shows

dispersion accuracy of the proposed fiber for fiber's global diameter change (d_1 , d_2 , and Λ) of order ± 1 , ± 2 and $\pm 5\%$ along with the optimum dispersion curve. It has been ensured that design accuracy of the fiber up to $\pm 2\%$ change in fiber's global diameter is within $0 \pm 2.0 \text{ ps/(nm-km)}$ maintaining dispersion flat characteristics.

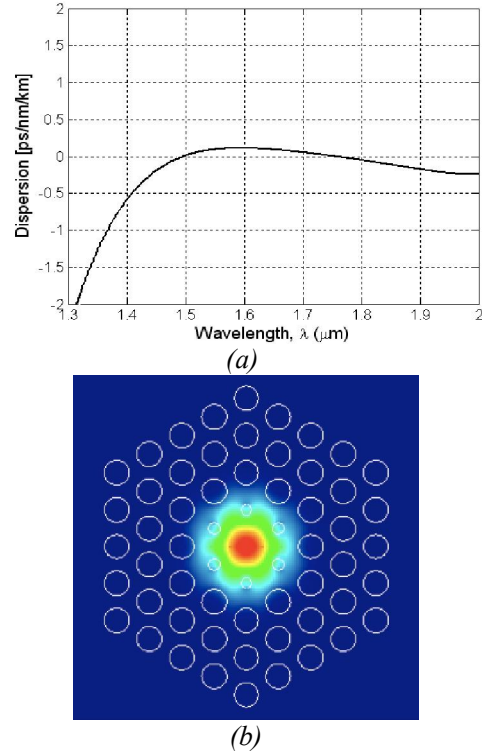


Fig. 7 (a) Optimum dispersion curve of the proposed DF-PCF for number of rings $N_r = 4$, $\Lambda = 1.70 \mu\text{m}$, $d_1/\Lambda = 0.30 \mu\text{m}$, and $d_2/\Lambda = 0.67 \mu\text{m}$. (b) Fundamental mode field distribution at $\lambda = 1.55 \mu\text{m}$.

Figure 10(a) shows effective areas of the fiber for optimum design parameters and also for global diameter variations of order 1 to $\pm 5\%$. The effective area of the fiber at $1.55 \mu\text{m}$ is $7.10 \mu\text{m}^2$. Nonlinear coefficient of the fiber corresponding to $7.10 \mu\text{m}^2$ is more than a $12 \text{ W}^{-1}\text{km}^{-1}$. Figure 10(b) shows confinement losses of the fiber for optimum design parameters and also for global diameter variations of order 1 to $\pm 5\%$. Confinement loss at $1.55 \mu\text{m}$ is 10^{-4} dB/m and is less than 10^{-3} dB/m below $1.70 \mu\text{m}$. Finally, a comparison is made between the DF-PCF and some other designs for ultra-flattened PCFs. Table 1 compares DF-PCF properties and some intriguing designs for ultra-flattened dispersion in the references

considering the ultra-flattened dispersion range, and number of design parameters including the number of rings layer. N_r , N_d , and N_d correspond to the number of rings, pitches, and air-hole diameters used in PCF design, respectively.

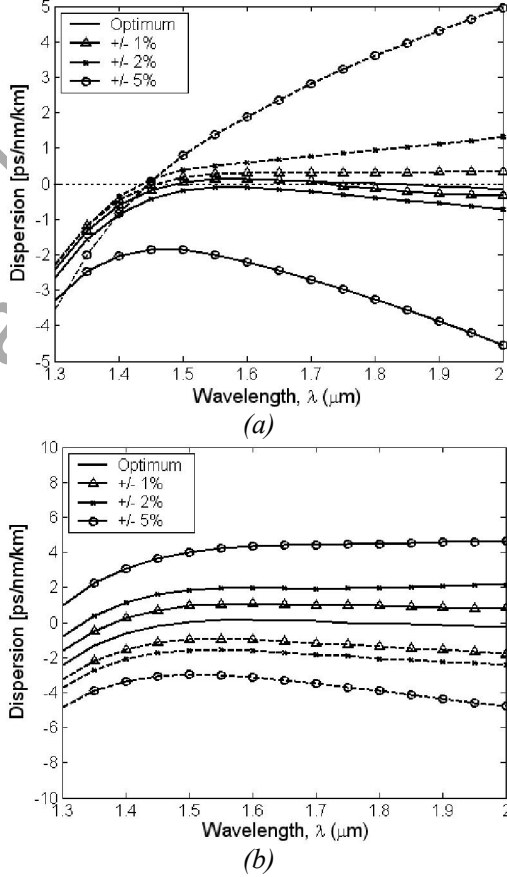


Fig. 8 Dispersion properties of the DF-PCF: (a) optimum dispersion and effects of changing d_1 , (b) optimum dispersion and effects of changing d_2 .

Although PCF in [10] is also attractive in the light of flat dispersion, its dispersion characteristic is more sensitive to variation in central defect air-hole diameter. On the other hand, the proposed DF-PCF has truly flat chromatic dispersion in the C and L band with low confinement loss and less design complexity, i.e., fewer design parameters as well as better fabrication tolerance to parameter variations. Therefore, the proposed fiber with a modest number of design parameters and novel dispersion properties may pave the way in different applications in nonlinear optics including optical parametric amplification, signal processing, soliton pulse

transmission, and supercontinuum generation in the infrared, and so on.

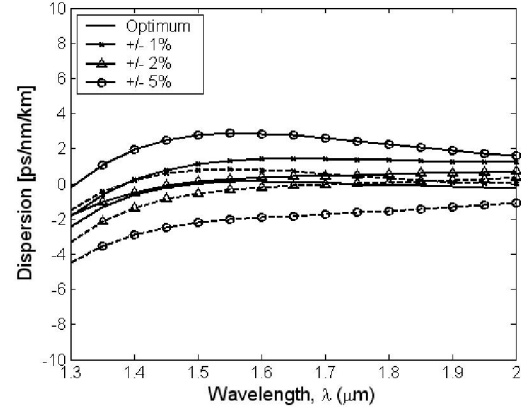


Fig. 9 Dispersion properties of the DF-PCF for fiber's global diameter variation of order 1 to $\pm 5\%$ around the optimum value (solid line).

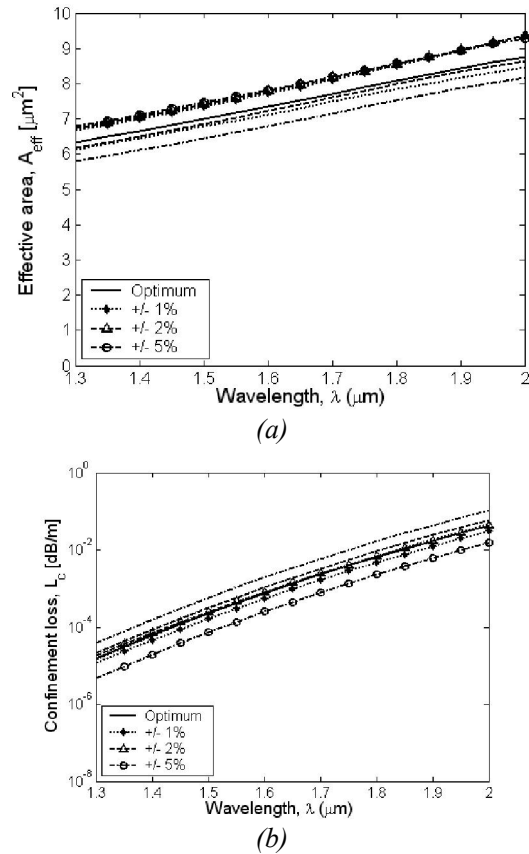


Fig. 10 (a) Effective areas and (b) Confinement losses of the proposed PCF for optimum design parameters and also for fiber's global diameter variations of order 1 to $\pm 5\%$ around the optimum value.

Table 1. Comparison of DF-PCF properties with some other remarkable designs

PCFs Design	$D(\lambda)$	1FDR (nm)	$^2NDP(N_r, N_d)$
Ref. [7]	0 ± 0.4	490	4, 1, 4
Ref. [8]	0 ± 1.2	600	11, 1, 1
Ref. [9]	0 ± 0.10	100	4, 1, 5
Ref. [10]*	0.2 ± 0.2	506	4, 1, 2
Ref. [11]	0 ± 0.50	430	4, 1, 2
Ref. [12]	0 ± 4.8	350	8, 2, 2
Ref. [14]	0 ± 1.0	543	–, 1, 1
Ref. [15]	0 ± 0.5	428	–, 1, 1
DF-PCF	$0 \pm 0.1/0 \pm 0.51$	300/600	4, 1, 2

¹FDR- flat dispersion range, ²NDP-number of design parameters,

*Defected core PCF.

IV. CONCLUSION

First, an octagonal PCF with ultra-flattened chromatic dispersion and low confinement loss has been reported. It has been shown through numerical simulation results that using a four-ring PCF, ultra-flattened dispersion is of 0 ± 0.50 ps/(nm-km) within a 1.31 to 1.70 μm wavelength range (390 nm band). Confinement loss is as low as 0.001 dB/km within a 1.31 to 1.65 μm wavelength ranges. Moreover, the proposed DF-OPCF shows better performance to variations in design parameters. Investigation based on O-PCF to obtain increased effective area dispersion flattened fiber is under study.

Second, a near zero truly ultra-flattened dispersion PCF has been presented with low confinement losses. It has been shown through numerical simulation results that a four ring PCF can assume near zero ultra-flattened dispersion of 0 ± 0.10 ps/nm/km in the wavelength range of 1.45 μm to 1.75 μm (300 nm) or, 0 ± 0.51 ps/nm/km in a 1.40 to 2.0 μm (600 nm) with low confinement loss of less than 10^{-3} dB/m below 1.70 μm . This fiber has a modest number of design parameters, two air-hole diameters and an air-hole pitch.

ACKNOWLEDGMENT

Thanks to Ministry of Science and Technology and Yoshinori Namhira's Laboratory for support and funding to this research works through 2.1/2013/DT-NDT Project.

REFERENCES

- [1]. X. Wang, K. Kikuchi, and Y. Takushima, Analysis of Dispersion-Managed Optical Fiber Transmission System Using Non-Return-to-Zero Pulse Format and Performance Restriction from Third-Order Dispersion, *IEICE Trans. Commun.*, vol. E82-B, pp.1141-1147, 1999.
- [2]. F. Futami, Y. Takushima, and K. Kikuchi, Generation of Wideband and Flat Supercontinuum over a 280-nm Spectral Range from a Dispersion-Flattened Optical Fiber with Normal Group-Velocity Dispersion, *IEICE Trans. Commun.*, vol. E82-B, pp.1265-1272, 1999.
- [3]. R. W. Tkach, A. R. Chraplyvy, F. Forghieri, A. H. Gnauck, and R. P. Derosier, *J. Lightwave Technol.*, vol. 13, pp. 841, 1995.
- [4]. J. J. Bernard, C. Brehm, J.-Y. Boniort, Ph. Dupont, J.-M. Gabriagues, C. Le Sergeant, M. Liegois, P. Francois, M. Monerie, and P. Sansonetti, *Ann. Telecommun.*, vol. 38, pp. 47, 1983.
- [5]. J.-S. Chiang and T.-L. Wu: "Analysis of propagation characteristics for an octagonal photonic crystal fiber (O-PCF)," *Optics Commun.*, vol. 258, no. 2, pp. 170-176, Feb. 2006.
- [6]. K. Kaneshima, Y. Namihira, N. Zou, H. Higa, and Y. Nagata: "Numerical investigation of octagonal photonic crystal fibers with strong confinement field," *IEICE Trans. Electron.*, vol. E89-C, no. 6, pp. 830-837, June 2006.
- [7]. K. Saitoh, M. Koshiba, T. Hasegawa, and E. Sasaoka: "Chromatic dispersion control in photonic crystal fibers: application to ultra flattened dispersion," *Opt. Express*, vol. 11, pp.843-852, May2003.
- [8]. W. H. Reeves, J. C. Knight, and P. St. J. Russell: "Demonstration of ultra-flattened dispersion in photonic crystal fibers," *Opt. Express*, vol.10, no.14, pp. 609-613, 2002.
- [9]. F. Poletti, V. Finazzi, T. M. Monro, N.G.R. Broderick, V. Tse, and D.J. Richardson, "Inverse design and fabrication tolerances of ultra-flattened dispersion holey fibers," *Opt. Express*, vol. 13, no. 10, pp. 3728-3736, May 2005.
- [10]. K. Saitoh, N.J. Florous, and M. Koshiba: "Ultra-flattened chromatic dispersion controllability using a defect-core photonic crystal fiber with low confinement loss," *Opt. Express*, vol. 13, no. 21, pp. 8365-8371, 2005.

- [11]. T. L. Wu and C. H. Chao, "A novel ultraflattened dispersion photonic crystal fiber," *IEEE. Photon. Technol. Lett.*, vol. 17, pp. 67-69, 2005.
- [12]. T. Matsui, J. Zhou, K. Nakajima, and I. Sankawa, "Dispersion-flattened Photonic Crystal Fiber with Large Effective area and Low Confinement Loss," *J. Lightwave Technology*, vol. 23, no. 12, pp. 4178-4183, Dec 2005.
- [13]. K. Saitoh and M. Koshiba, "Highly nonlinear dispersion-flattened photonic crystal fibers for supercontinuum generation in the telecommunication window," *Opt. Express*, vol. 12, no. 10, pp. 2027-2032, May 2004.
- [14]. A. Ferrando, E. Silvestre, P. Andres, J. J. Miret, and M. Andres: "Nearly zero ultraflattened dispersion in photonic crystal fibers," *Opt. Lett.*, vol. 25, no. 11, pp. 790-792, June 2000.
- [15]. A. Ferrando, E. Silvestre, P. Andres, J. Miret, and M. Andres: "Designing the properties of dispersion-flattened photonic crystal fibers," *Opt. Express*, vol. 9, no. 13, pp. 687-697, Dec. 2001.
- [16]. Shangping Guo, Feng Wu, Sacharia Albin, Hsiang Tai, and R. S. Rogowski, "Loss and dispersion analysis of micro structured fibers by finite difference method," *Opt. Express*, vol. 12, no. 15, pp. 3341-3352, July 2004.
- [17]. G. Renversez, B. Kuhlmeier, and R. McPhedran, "Dispersion management with microstructured optical fibers: ultraflattened chromatic dispersion with low loss," *Opt. Lett.*, vol. 28, no. 12, pp. 989-991, June 2003.
- [18]. S. G. Leon-Saval, T. A. Birks, N. Y. Joly, A. K. George, W. J. Wadsworth, G. Kakarantzas, and P. St. J. Russell, "Splice-free interfacing of photonic crystal fibers," *Opt. Lett.*, vol. 30, no. 13, pp. 1629-1631, 2006.
- [19]. Crystal Fiber A/S. <http://www.crystal-fiber.com>.

AUTHOR' BIOGRAPHY



Nguyen Hoang Hai received a B.E. degree in Electronics and Telecommunication Engineering from Hanoi University of Technology (HUT) in 1999. In October 2000, he joined the Department of Electrical and Electronics Engineering at the University of the Ryukyus, Okinawa, Japan as a graduate

student, where he worked in the field of Microwave Circuit Elements, Electromagnetic Theory. Since Oct 2006, he has been with the Department of Electrical and Electronics Engineering at University of the Ryukyus, Okinawa, Japan as a Doctoral student.

He received his Doctor degree in 2009 in nonlinear

photonic crystal for optical communication system. He is working in the Department of Telecommunication System, School of Electronics and Telecommunication, Hanoi University of Science and Technology.

His current research interest include Photonic Switching, Photonic Crystal and Highly Nonlinear Optic for medical application, optical coherent tomography (OCT). He is a member of the Institute of Electrical Electronics Engineering (IEEE), and the Institute of Electronics Information, and Communication Engineering (IEICE).